Physica B 414 (2013) 35–41

Contents lists available at SciVerse ScienceDirect

Physica B

journal homepage: www.elsevier.com/locate/physb

Temperature dependent I–V characteristics of an Au/n-GaAs Schottky diode analyzed using Tung's model

Demet Korucu [a], Abdulmecit Turut [b,*], Hasan Efeoglu [c]

[a] Hakkari University, Faculty of Engineering, Department of Material Science and Engineering, TR-30000 Hakkari, Turkey
[b] Istanbul Medeniyet University, Faculty of Sciences, Department of Physics Engineering, TR-34730 Istanbul, Turkey
[c] Atatürk University, Faculty of Engineering, Department of Electrical and Electronics Engineering, TR-25240 Erzurum, Turkey

ARTICLE INFO

Article history:
Received 6 October 2012
Received in revised form
22 December 2012
Accepted 3 January 2013
Available online 17 January 2013

Keywords:
GaAs semiconductor
Schottky diodes
Schottky barrier height
Barrier inhomogeneity
Richardson constant
Metal–semiconductor–metal contacts

ABSTRACT

The current–voltage (*I–V*) characteristics of Au/n-GaAs contacts prepared with photolithography technique have been measured in the temperature range of 80–320 K. The ideality factor and barrier height (BH) values have remained almost unchanged between 1.04 and 1.10 and at a value of about 0.79 eV at temperatures above 200 K, respectively. Therefore, the ideality factor values near unity say that the experimental *I–V* data are almost independent of the sample temperature, that is, contacts have shown excellent Schottky diode behavior above 200 K. An abnormal decrease in the experimental BH Φ_b and an increase in the ideality factor with a decrease in temperature have been observed below 200 K. This behavior has been attributed to the barrier inhomogeneity by assuming a Gaussian distribution of nanometer-sized patches with low BH at the metal-semiconductor interface. The barrier inhomogeneity assumption is also confirmed by the linear relationship between the BH and the ideality factor. According to Tung's barrier inhomogeneity model, it has been seen that the value of σ_T=7.41 × 10^{-5} cm$^{2/3}$ V$^{1/3}$from ideality factor versus $(kT)^{-1}$ curve is in close agreement with σ_T=7.95 × 10^{-5} cm$^{2/3}$ V$^{1/3}$ value from the $\Phi_{\rm eff}$ versus $(2kT)^{-1}$ curve in the range of 80–200 K. The modified Richardson $\ln(J_0/T^2)-(q\sigma_T)^2(V_b/\eta)^{2/3}/[2(kT)^2]$ versus $(kT)^{-1}$ plot, from Tung's Model, has given a Richardson constant value of 8.47 A cm^{-2} K^{-2}which is in very close agreement with the known value of 8.16 A cm^{-2} K^{-2} for n-type GaAs; considering the effective patch area which is significantly lower than the entire geometric area of the Schottky contact, in temperature range of 80–200 K. Thus, it has been concluded that the use of Tung's lateral inhomogeneity model is more appropriate to interpret the temperature-dependent *I–V* characteristics in the Schottky contacts.

1. Introduction

The metal–semiconductor (MS) rectifying contacts play an important role in integrated circuit technology [1–5]. The Schottky diodes (SDs) often generally give non-ideal current–voltage (*I–V*) characteristics at low temperatures, even if the diode exhibits an ideal behavior at temperatures around room temperature [6–20]. Many researchers have attributed the temperature dependence of Schottky barrier height (SBH) in MS contacts to the spatial inhomogeneities barrier and they have interpreted this behavior by regarding thermionic emission (TE)-diffusion mechanism with a Gaussian distribution (GD) of barrier heights (BHs) [6–23]. Talin et al. [19] have measured the nanometer-resolved lateral variations in the BH using the ballistic electron emission microscopy (BEEM) and have compared the spatial profile and the statistical distribution of the BHs of Au/n-GaAs contacts to the macroscopic BH obtained from the *I–V* and capacitance–voltage (*C–V*) characteristics of the same MS contact. First of all, Song et al. [9] have indicated that the variations of the SBH over the contact area in SB contacts can occur as a result of inhomogeneities in the interfacial oxide layer composition, non-uniformity of the interfacial layer thickness, and distributions of interfacial charges. They [9] have obtained reasonable values of the effective Richardson constant (RC) by taking account for temperature coefficient of BH and using a modified TE expression for the *I–V* characteristics by considering the GD of the temperature-dependent BHs over the contact area.

Werner and Guttler [10] have suggested a new analytical potential fluctuations model for the interpretation of *I–V* and *C–V* measurements on spatially inhomogeneous Schottky contacts or on a continuous spatial distribution of the current barriers and have used the PtSi/Si data in order to exemplify the evaluation on the basis of their model. They [10] have determined the

* Corresponding author. Tel.: +90 216 280 33x33; fax: +90 216 602 28.
E-mail addresses: amecit2002@yahoo.com, aturut@medeniyet.edu.tr (A. Turut).

0921-4526/$ - see front matter © 2013 Elsevier B.V. All rights reserved.
http://dx.doi.org/10.1016/j.physb.2013.01.010

temperature-dependent differences of capacitance and current barriers by a value which depends on the standard deviation of the distribution, and used a plot of the zero-bias values ($\Phi_b^c - \Phi_{ap}$) versus inverse temperature to determine the zero-bias standard deviation, where Φ_{ap} is the zero bias apparent BH of the current barrier, the capacitance barrier Φ_b^c is equal to the mean barrier $\overline{\Phi}_{bo}$ of the current barrier distribution. According to Werner and Guttler's approach, it has been also required the experimental C–V data for determining the temperature-dependent differences of capacitance and current barriers, and the zero-bias standard deviation.

Sullivan et al. [11] and Tung [12] have showed that non-ideal behavior of the SBDs could be quantitatively explained by assuming a distribution of nanometer-scale interfacial patches of reduced SBH. They [11,12] have depicted an inhomogeneous contact as a distribution of small regions, so-called patches, with different low BH values than the junction's main barrier. However, Werner and Guttler [10] and Sullivan et al. [11] and Tung [12] have not introduced any suggestion about how to determine RC value of the semiconductor in a MS contact using their own approaches. Chand and Kumar [13] have interpreted the I–V characteristics of Pd_2Si based Schottky diodes on both n- and p-type silicon measured over a wide temperature on the basis of TE-diffusion mechanism and the assumption of a Gaussian distribution of BHs by following Song et al. [9] and Werner and Guttler [10]. They [13] directly used a plot of the Φ_{ap} versus inverse temperature to determine zero-bias standard deviation and the mean barrier $\overline{\Phi}_{bo}$of the current BHs without requiring the experimental C–V data, and they have modified the conventional activation energy equation under the assumption of GD of BHs. That is, for determining RC, the modified Richardson (MR) $\ln(I_0/T^2) - q^2\sigma_0^2/2k^2T^2$ versus (T^{-1}) plot from distribution parameters has been used by Chand and Kumar [13] to modify the experimental data, where σ_0 is the zero-bias standard deviation, I_0 is the saturation current and T is the absolute temperature.

Furthermore, Iucolano et al. [14] and Roccaforte et al. [15] have investigated the temperature dependence of the electrical properties of Pt/GaN and Ni_2Si/4H-SiC SBDs, respectively, and have argued that the underestimation of the RC value can be related to the formation of a laterally inhomogeneous Schottky barrier which may result into an effective area for the current conduction lower than the total area of the diode, and they [14,15] have obtained the correct value of the RC value from the MR plot using the different values of A_{eff} at the different temperatures in terms of Tung's model, i.e., $\ln[I_0/(A_{\text{eff}}T^2)]$ versus $(nT)^{-1}$ or $\ln[I_0/(NA_{\text{eff}}T^2)]$ versus $(T)^{-1}$ plot, respectively, where A_{eff} is the effective area of a patch with low SBH, and the product NA_{eff} represents the total effective area of the patches contributing to the current transport. Kumar et al. [16] have studied to determine the value of the RC value in the indium nitride nanodot-silicon (InN ND-Si) heterostructure SBDs in terms of Tung's model by following Roccaforte et al. [15]. Recently, for Mo/p-GaTe SBDs, Gulnahar and Efeoglu [17] have aimed to obtain the value of the RC from the MR plot using the different values of standard deviation at the different temperatures in terms of Werner and Guttler's approach [10]. Soylu and Yakuphanoglu [18] have performed a statistical study on the experimental BHs and ideality factors of forward bias I–V characteristics of Au/n-GaAs diodes at room temperature. They show that the current expression for inhomogeneous Schottky contacts by Sullivan et al. [11] and Tung [12] exhibits an excellent fit to the experimental I–V curve at room temperature.

We have measured the I–V characteristics of Au Schottky contacts on an n-GaAs substrate in the temperature range of 80–320 K. The temperature-dependent barrier characteristics of the Au/n-GaAs Schottky contacts have been interpreted by the modified TE model taking into account the possible presence of a distribution of nanometer-sized "patches" with lower BH embedded in a uniform high barrier background suggested by Sullivan et al. [11] and Tung [12]. To the best of our knowledge there has been no report on the modified Richardson plot from the I–V characteristics of the ideal Schottky contacts using Tung's patch model. As different from studies above, we will study to obtain the RC value from the MR $\ln[I_0/(NA_{\text{eff}}T^2)]\ (q\sigma_T)^2(V_b/\eta)^{2/3}/[2(kT)^2]$ versus $(kT)^{-1}$ plot for the Au/n-GaAs SBDs according to the GD of BHs in terms of Tung's model. If I–V characteristics of a SBD obey the TE model, the BH of such a diode is frequently laterally homogeneous, the diode exhibits approximately an ideal behavior at temperatures around room temperature and offers to calculate the expected diode parameters for a test of the validity of theories of the Schottky barrier.

2. Experiment details

The Au/n-GaAs SBDs were fabricated using n-type single crystals n-GaAs wafer with (1 0 0) surface orientation, having 300 μm thickness and 7.3×10^{15} cm^{-3} carrier concentration. The GaAs wafer was degreased for 5 min in organic solvent of trichloroethylene, acetone and methyl alcohol and was etched in a sequence of sulfuric acid and hydrogen peroxide, 20% hydrofluoric acid (HF, a solution of nitric acid (6 HNO_3): 1HF:35 H_2O, 20% HF and finally quenched in de-ionized water of resistivity of 18 MΩ cm. During each cleaning step, the wafer was rinsed thoroughly in de-ionized water of resistivity of 18 MΩ. Then, low resistance ohmic contacts to n-GaAs wafer was made by using high purity (99.999%) Al with a thickness of about 2000 Å, Al was evaporated onto whole back side of n-GaAs wafer in high vacuum system of 10^{-6} Torr. The ohmic contacts were annealed by a temperature treatment at 425 °C for 3 min. For Schottky contacts, the n-GaAs wafer was placed on a rotating table which is rotated at a fixed rotational speed with 5000 rpm for 45 s using with positive photoresist (AZ5214). After this process, UV light was used to cure the resist into the desired structural pattern using a photo mask for 90 s. The photoresist was then developed 60 s, with the exposed regions dissolving in the solvent. Finally the photoresist was removed for 3 min by acetone and dried with N_2. The Schottky contacts were formed by photolithography process of Au dots diameters of 200 μm onto the front surface through a photomask (the diode area is 3.14×10^{-4} cm^2).

The current–voltage (I–V) characteristics of Au/n-GaAs SBDs were performed by using a Keithley 2400 Sourcemeter. All measurements were carried out in the temperature range of 80–320 K using a temperature controlled Janes vpf-475 cryostat, which enables us to make measurements in the temperature range of 77–450 K. The bias voltage is swept from 0.0 to +1.0 V. The sample temperature was always monitored by use of a copper-constant thermocouple close to the sample and measured with a Keithley model 199 DMM/scanner and Lakeshore model 321 auto-tuning temperature controllers with sensitivity better than ±0.1 K.

3. Results and discussion

The electrical I–V measurements of the device were made in the temperature range of 80–320 K. The current through a uniform metal–semiconductor interface due to thermionic emission can be expressed as [1]:

$$I = I_0 \exp\left(\frac{qV}{nkT}\right)\left[1 - \exp\left(-\frac{qV}{kT}\right)\right] \tag{1}$$

where I_0 is the saturation current given by

$$I_0 = AA^*T^2\exp\left(-\frac{q\Phi_{ap}}{kT}\right), \tag{2}$$

where q is the electron charge, V is the forward-bias voltage, A is the effective diode area, k is the Boltzmann constant, T is the absolute temperature, A^* is the effective Richardson constant (RC) of 8.16 A cm^{-2} K^{-2} for n-type GaAs, Φ_{ap} is the zero bias apparent barrier height (BH) and n is the ideality factor. From Eq. (1), ideality factor n can be written as

$$n = \frac{q}{kT}\left(\frac{dV}{d\ln I}\right) \tag{3}$$

The ideality factor, n, is introduced to take into account the deviation of the experimental I–V characteristics from the ideal thermionic model and should be $n=1$ for an ideal contact. Fig. 1 shows the semilog-forward bias I–V characteristics of the Au/n-GaAs Schottky contact in the temperature range of 80–320 K.

The experimental values of the BH Φ_{ap} and ideality factor n for the device were determined from intercepts and slopes of the forward-bias ln$I$ versus V plot at each temperature, respectively. The experimental values of Φ_{ap} and n range from 0.79 eV and 1.034 (at 320 K) to 0.59 eV and1.53 (at 80 K), respectively. Fig. 2 shows the values of Φ_{ap} and n as a function of temperature. At temperatures below 200 K, the experimental values of n increased and Φ_{ap} decreased with a decrease in temperature, as can be seen from Fig. 2.The ideality factor values of the device have remained almost unchanged between 1.04–1.10 in the temperature range of 190–320 K, and BH has remained constant at a value of about 0.79 eV in the temperature range of 190–320 K. Therefore, it can be said due to the ideality factor values near unity that the experimental I–V data are almost independent of the sample temperature and quite well obey the TE model over whole bias range at temperatures above 190 K.

The temperature dependence of the ideality factor n of the SBDs can be expressed in the form

$$n = 1 + \frac{T_0}{T} \tag{4}$$

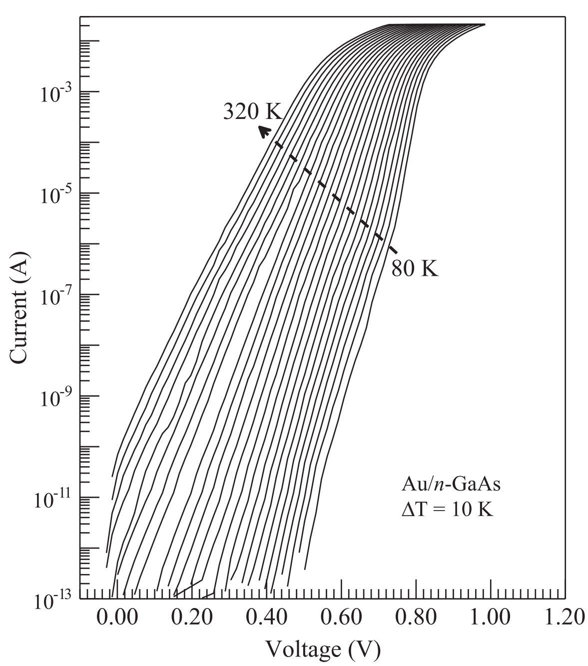

Fig. 1. Experimental forward bias current–voltage characteristics of the Au/n-GaAs Schottky Barrier Diode in the temperature range of 80–320 K.

where T_0 is a constant called the excess temperature. This behavior is commonly accepted as the "T_0 anomaly," is a direct consequence of a real Schottky contact with a distribution of barrier inhomogeneities. Fig. 3 shows the experimental nT versus T plot of the Au/n-GaAs in temperature ranges of 80–320 K. A value of T_0=10.33 K was obtained from the experimental nT versus T plot in the temperature range of 200–320 K. The value of T_0=10.33 K says that the current across diode quite well obeys the TE model at temperatures above 190 K. There is a deviation from ideality below 190 K. The linear fit to the experimental data at low temperatures in Fig. 3 gives a value of T_0=41.60 K, as can be seen from Fig. 3. These findings can be satisfactorily explained by the concept of the barrier inhomogeneities, indicating that the current through small and low BH regions in the MS contacts should be a strong function of the spatial dimensions of the low BH regions. The inhomogeneity of a real MS contact may cause anomalous I–V behavior and the strong temperature dependence of the apparent SBH and ideality factor deduced from I–V data at low temperatures. At low temperatures and in the low bias region, the I–V characteristics may be dominated by a few large

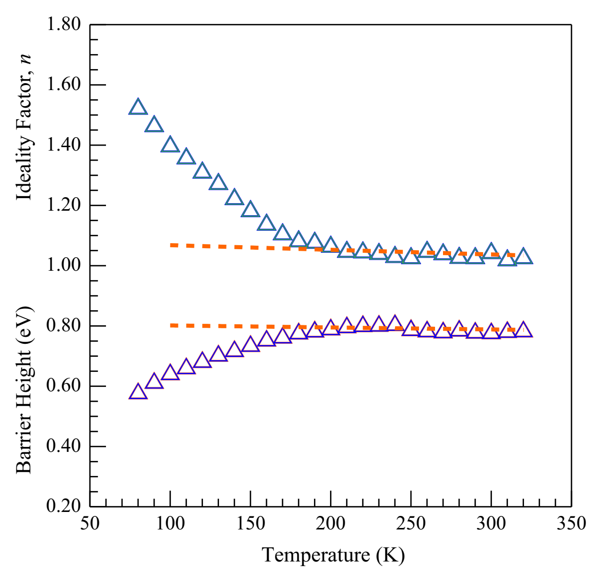

Fig. 2. The barrier height and ideality factor plots in the temperature range of 80–320 K.

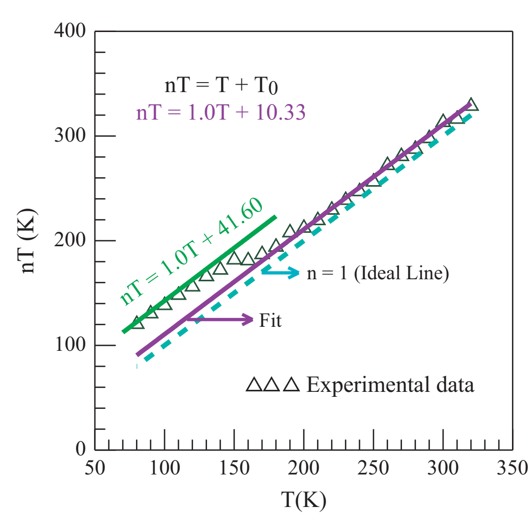

Fig. 3. Experimental nT versus T plot in the temperature range of 80–320 K.

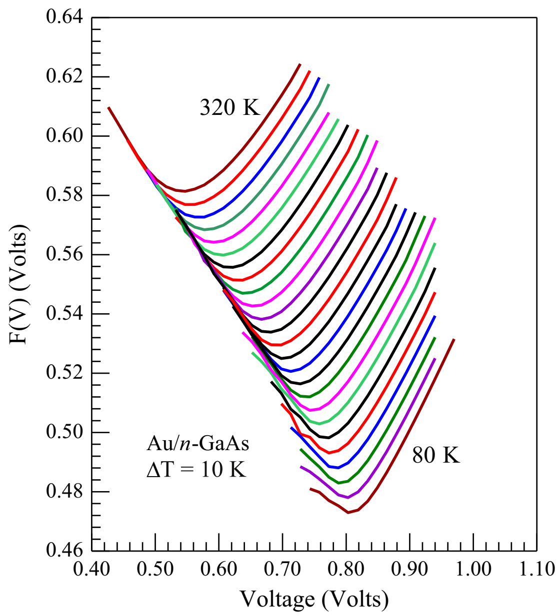

Fig. 4. $F(V)$ versus V plot determined by means of Norde's Model using the I–V data at various temperatures in Fig. 1.

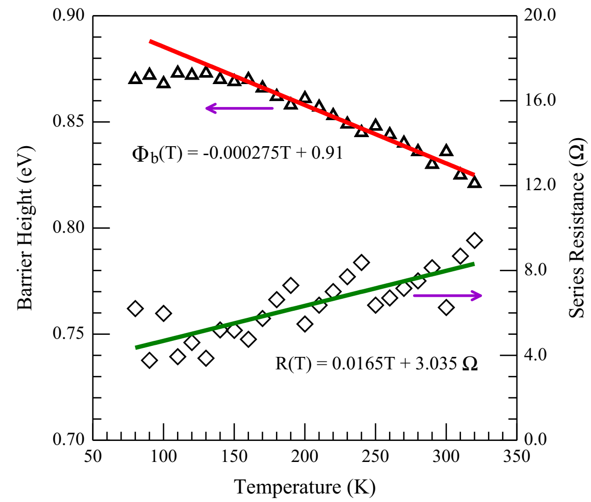

Fig. 5. Temperature dependence of the barrier height and series resistance determined from the curves in Fig. 4 by Norde's functions.

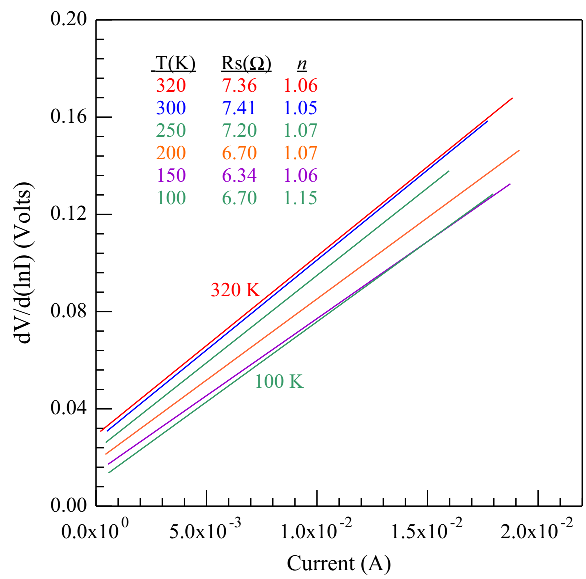

Fig. 6. $d(V)/d(\ln I)$ versus current plots by Cheung's Model for determination of the series resistance at different temperatures.

patches with low barriers. At high temperatures or in the large bias region at low temperatures, the total current is dominated by a large number of small patches, which can be approximately described as a Gaussian distribution of the barrier heights [22–29].

Norde [30] proposed a function $F(V)$ to determine value of the series resistance by considering Eq. (1):

$$F(V)=\frac{V}{\gamma}-\frac{kT}{q}\ln\left(\frac{I(V)}{AA^{*}T^{2}}\right) \tag{5}$$

where the current $I(V)$ is obtained from the I–V curves at each temperature in Fig. 1. Fig. 4 shows the$F(V)$ versus V plots obtained using the I–V data in Eq. (5). The BH relation can be given as follows [30]

$$\Phi(T)=F(V_{\min})+\frac{V_{\min}}{2}-\frac{kT}{q}. \tag{6}$$

where $F(V_{\min})$ is the minimum value of $F(V)$ and the corresponding voltage is $V_{\min}$. The series resistance R_s can be expressed as [30]

$$R_s=\frac{(2-n)kT}{qI_{\min}} \tag{7}$$

where $I_{\min}$ is the value of the forward current at the voltage $V_{\min}$ where the function $F(V)$ exhibits a minimum. The series resistance values from the $F(V)$–V curves as a function of temperature are given in Fig. 5 (indicated by open squares). The series resistance values vary from 9.42 Ω at 320 K to 6.21 Ω at 80 K. The fit to the R_s values in Fig. 5 gives a straight line with the slope of 0.0165 Ω K^{-1} in the temperature range of 80–320 K. Therefore, it can be said that the series resistance is almost independent of the temperature. This result is also confirmed by the series resistance values obtained for different temperatures using Cheung's functions [31] in Fig. 6. The resistance values in Fig. 6 vary from 7.36 Ω at 320 K to 6.70 Ω at 100 K. However, at first sight, the 'Cheung' 100 K value $n=1.15$ (Fig. 6) seems to deviate from the 'standard' 100 K value $n=1.4$ (Figs. 2 and 3). The extracted parameters generally depend on the method used and must be carefully considered in order to get reliable and accurate evaluation of the parameters [32,33]. Good linearity of the plots obtained by Cheung's functions provides that the parameters by Cheung's method become reliable and accurate and minimizes the specific errors caused by the series resistance [32]. The ideality factor directly calculated from the forward bias I–V plots in Fig. 1 by Eq. (3) is voltage-dependent which can be caused by the contribution of different carrier transport mechanisms and by the strong influence of the series resistance. The main disadvantages of Norde's method are that the ideality factor is assumed to be very close to unity which is not always true for a real diode and that only a single point of I–V characteristic is used to calculate the BH and series resistance. These problems often lead to a series resistance value larger than expected. These methods use plots of auxiliary functions to evaluate the diode parameters more accurately. However, the methods have their own weaknesses as well [32,33].

The BH versus temperature plot obtained by Norde's method for the Au/n-GaAs SBD is given in Fig. 5 (indicated by open triangles). As essentially indicated above, Norde's method is used to determine the value of the BH in the case where the thermionic emission dominates. In addition, the temperature coefficient of the BH can be determined using Norde's method. The temperature dependence of the BH can be expressed as

$$\Phi(T) = \Phi(T=0) - \alpha T \tag{8}$$

where $\Phi(T)$ values are determined from the $F(V)$ versus V plot using Eq. (6). As seen from Fig. 5, the BH value has increased as linear with a decrease in temperature at the temperature above 150 K, but almost unchanged at temperatures below 160 K. In Fig. 5, the fitting to $\Phi(T)$ data according to Eq. (6) yields a straight line with the slope of $\alpha = -0.275$ meV K^{-1} which is called the temperature coefficient value of the BH. Missous et al. [34] have obtained the values of -0.23 ± 0.03 and -0.32 ± 0.03 meV K^{-1} from the C^{-2}–V–T characteristics for Au/n-GaAs and Al/n-GaAs SBDs, respectively. These values [34] are in close agreement with the value obtained by us within the experimental uncertainty. However, Passler [35], Thurmond [36] and Lautenschlager et al. [37] indicated the values of -0.472, 0.5405 and 0.55 meV K^{-1} for the temperature coefficient of the energy band gap of n-type GaAs, respectively. The variation of the BH value with temperature is normally explained within the frame of the Fermi level pinning concept due to the temperature-dependent variation in the band gap [38]. The temperature coefficient of BH obtained by us is approximately equal to half of the temperature coefficient of the energy gap of n-type GaAs.

Fig. 7 shows the Richardson plot in temperature range of 80–320 K. As mentioned above, the ideality factor values near unity says that the experimental I–V data are almost independent of the sample temperature and quite well obey the standard TE current model over whole bias range at temperatures above 200 K. The fit to the data which obeys the standard TE current model in Fig. 7 gives a straight line in the temperature range of 200–320 K. The y-axis intercept and slope of the Richardson plot in the temperature range of 200–320 K will give a RC value of 8.30 A cm^{-2} K^{-2}, and an effective barrier height of 0.81 eV, respectively. The RC value of 8.30 A cm^{-2} K^{-2} for the range of 200–320 K is very close to 8.16 A cm^{-2} K^{-2} known for electrons in n-type GaAs.

As can be seen from Figs. 2 and 8, at low temperatures below 200 K, both the BH and n values are strongly dependent on temperature. The decrease in the BH value with decreasing temperature can be explained by the concept of lateral barrier inhomogeneity, introducing a TE mechanism with Gaussian distribution function of the barrier heights suggested by Sullivan et al. [11] and Tung [12]. The nanoscale measurements made by Iucolano et al. [14] demonstrated a GD of the barrier height along the metal/GaN interface. The barrier inhomogeneity assumption was also confirmed by the linear relationship between the barrier height and the ideality factor (Fig. 8). As can be seen from Fig. 8, the barrier height increases the ideality factor decreases with an increase in the measurement temperature. Such a temperature dependent of the barrier height and ideality factor observed in "real" Schottky barriers may be attributed to the inhomogeneity of the contact [39–41].The extrapolation at $n=1$ of the BH versus n plot showing a linear correlation between both of these parameters gives a value barrier height of 0.83 eV.

To explain commonly observed deviations from the standard TE theory, Tung describes an inhomogeneous contact as a distribution of regions "nanometer-sized patches" with different low barrier height values and areas embedded in a uniform higher Schottky barrier area. The inhomogeneities may play an important role in the determination of the experimental data and have to be considered in the evaluation of experimental I–V characteristics. The application of standard procedures (Eq. (1)) gives the effective BH and ideality factors only. For small and circular patches, assuming a Gaussian distribution of low-SBH circular patches characterized by a distribution with standard deviation σ_T, Tung has given the modified TE expression of the forward bias current. Now, let us study to explain the above abnormal behaviors using a barrier potential fluctuation model based on spatially inhomogeneous BHs at the interface given by Sullivan et al. [11] and Tung [12]. Thus, the modified saturation current can be written as

$$I_0 = NA_{\mathrm{eff}}A^*T^2 \exp\left[-\frac{q}{kT}\left(\Phi_{b0}^{\mathrm{hom}} - \frac{\sigma_T^2}{2kT}\left(\frac{V_{b0}}{\eta}\right)^{2/3}\right)\right] \tag{9}$$

where

$$\Phi_{\mathrm{eff}} = \Phi_{b0}^{\mathrm{hom}} - \frac{\sigma_T^2}{2kT}\left(\frac{V_{b0}}{\eta}\right)^{2/3} \tag{10}$$

the experimentally apparent or effective BH measured from the forward bias I–V characteristics,Φ_{bo}^{hom} is the homogeneous barrier height, $\eta = \varepsilon_s\varepsilon_o/qN_d$, ε_s and N_d are the dielectric constant and the dopant density of the semiconductor substrate. It can obviously be seen from the equations above that the effective BH depends on the bias and temperature. N is the number of patches covering area of the diode as free parameter, A_{eff} is the effective area of a patch with low SBH, that is, involved effective area of the patches in the current transport at low temperatures, and the product

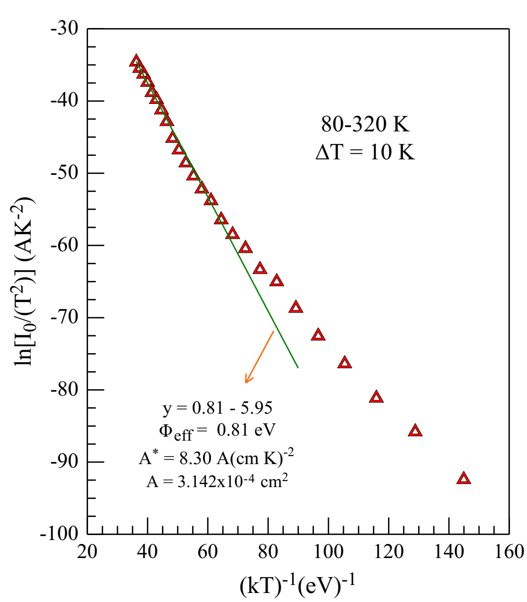

Fig. 7. Richardson plot in temperature range of 80–320 K. The solid line represents a straight linear fit at the higher temperature data (200–320 K).

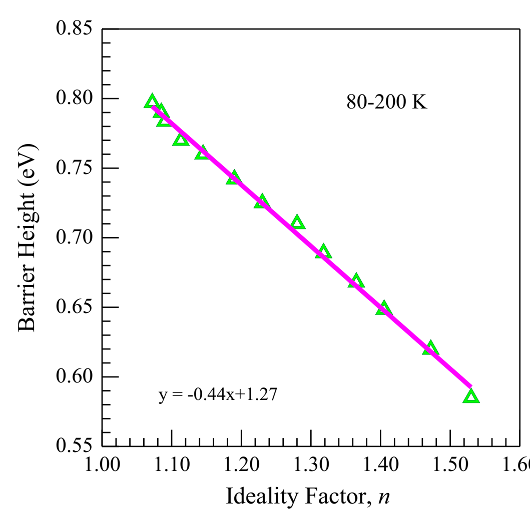

Fig. 8. Apparent barrier height versus apparent ideality factor in temperature range of 80–200 K.

NA_{eff} represents the total effective area of the patches contributing to the current transport. Obviously, although N is independent of temperature, as it gives the number of patches in the contact, the product (NA_{eff}) exhibits a temperature dependency, V_{b0} is the zero bias interface band bending of the uniform barrier outside the patch [11,12]. Furthermore, A_{eff} can be also expressed as [12]

$$A_{eff} = \frac{8\pi(2kT)}{9}\left(\frac{\eta}{V_{b0}}\right)\left(\Phi_{b0}^{hom} - \Phi_{eff}\right) \quad (11)$$

To obtain the modified Richardson plot by means of Eq. (9), it should be found σ_T value by plotting Φ_{eff} versus $(2kT)^{-1}$ curve in accordance with Eq. (10). The linear plot in Fig. 9 gives a value$\sigma_T = 7.95\times10^{-5}$ cm$^{2/3}$ V$^{1/3}$ in the range of 80–200 K. The values of A_{eff} were determined from Eq. (11) at each temperature, for example, the value of $A_{eff} = 2.00\times10^{-11}$ cm^2 at 200 K, and 2.24×10^{-11} cm^2 at 80 K.

Moreover, for the modified TE current expression described by Tung's model [12], the ideality factor is given by

$$n \approx 1 + \frac{\sigma_T^2 V_{b0}^{-1/3}}{3kT\eta^{2/3}} \quad (12)$$

Fig. 10 shows the apparent ideality factor versus $(kT)^{-1}$ curve, according to Tung's Model in temperature range of 80–200 K, that is, Fig. 10 shows the same data as shown in a part of Fig. 3. The linear fit to the experimental data in Fig. 10 gives a value of $\sigma_T = 7.41\times10^{-5}$ cm$^{2/3}$ V$^{1/3}$ in the range of 80–200 K. This value approximately is the same as $\sigma_T = 7.95\times10^{-5}$ cm$^{2/3}$ V$^{1/3}$ value from the Φ_{eff} versus $(2kT)^{-1}$ curve in the same temperature range. When Eq. (4) has been compared with Eq. (12), T_0 can be expressed as

$$T_0 = \frac{\sigma_T^2}{3kV_{b0}^{1/3}\eta^{2/3}} \quad (13)$$

A value of $T_0 = 39.32$ K is obtained using $\sigma_T = 7.41\times10^{-5}$ cm$^{2/3}$ V$^{1/3}$ value in Eq. (13). This value is in close agreement with the value of $T_0 = 41.60$ K found by the linear fit to the experimental data at low temperatures in Fig. 3.

From Eq. (9), the modified Richardson expression can be written as

$$\ln\left(\frac{I_0}{NA_{eff}T^2}\right) - \frac{\sigma_T^2(V_{b0})^{2/3}}{2(kT)^2\eta^{2/3}} = \ln(A^*) - \frac{\Phi_{b0}^{hom}}{kT} \quad (14)$$

Fig. 11 shows the modified Richardson $\ln(J_0/T^2)\ (q\sigma_T)^2(V_b/\eta)^{2/3}/[2(kT)^2]$ versus $(kT)^{-1}$ curve for the Au/n-GaAs Schottky contact according to the GD of BHs by considering Tung's model in the temperature range of 80–200 K. The full line in Fig. 11 displays the fit of Eq. (14) to the experimental data. As stated above, N is the number of patches covering area of the diode as free parameter. The product NA_{eff} may be accepted as an average total effective area of the patches contributing to the current transport. We taken as $N = 3.25\times10^4$ which gives a good fit to the experimental data in $\ln(J_0/T^2)\ (q\sigma_T)^2(V_b/\eta)^{2/3}/[2(kT)^2]$ versus $(kT)^{-1}$ curve in Fig. 11. Thus, $NA_{eff} = 6.49\times10^{-7}$ at 200, and 7.28×10^{-7} cm^2 at 80 K. These values at 200 and 80 K correspond to only about 0.21% and 0.23% of the entire geometric area of the Schottky contact, respectively. Thus, it has been seen that the effective area involved in the current transport is significantly lower of the entire geometric area of the Schottky contact. A RC of 8.47 A cm^{-2} K^{-2}was obtained from Fig. 7. This approximately is in close agreement with the value of 8.16 A cm^{-2} K^{-2} given for electrons in n-type GaAs. Furthermore, the lateral homogeneous BH value of 0.84 eV is in close agreement with the lateral homogeneous BH value of 0.83 eV from the BH versus ideality factor plot in the temperature range of 80–200 K.As can be seen from the calculations above, according to Tung's model, a RC

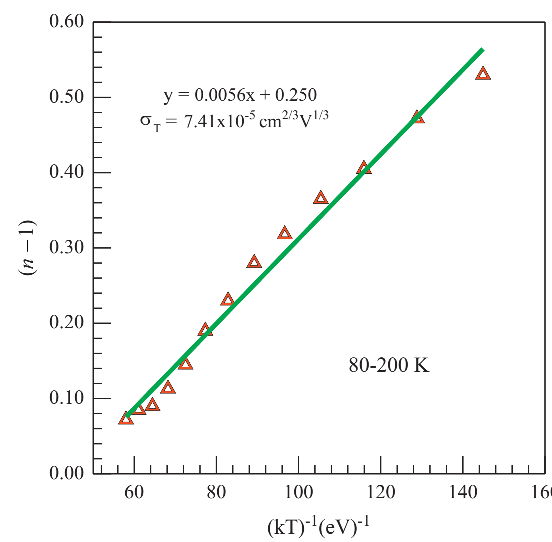

Fig. 10. Apparent ideality factor versus $(kT)^{-1}$ curve according to Tung's model in temperature range of 80–200 K.

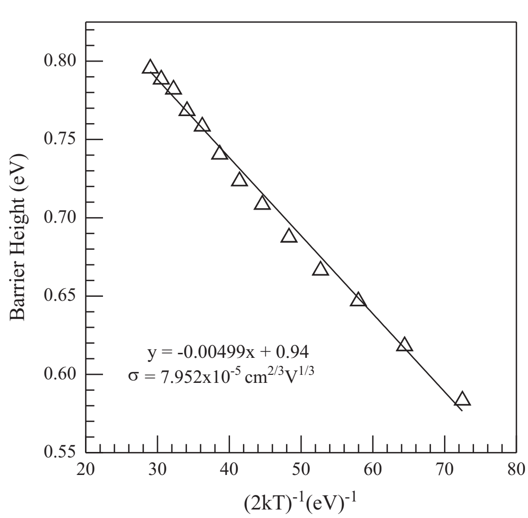

Fig. 9. Apparent barrier height versus $(2\,kT)^{-1}$ plot according to Tung's model in temperature range of 80–200 K.

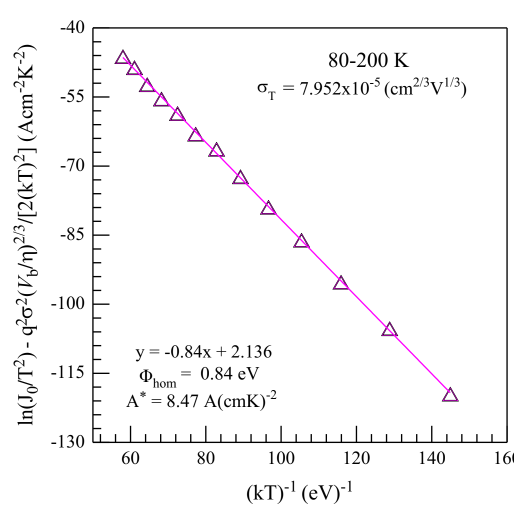

Fig. 11. Modified Richardson plot according to Tung's model in temperature range of 80–200 K.

value to close the theoretical value can be obtained from the modified Richardson plot. This is ascribed to the fact that an effective area lower than the geometric area of the device has been used in the calculations, this is involved effective area of the patches in the current transport at low temperatures. Such an effective area for the device is supplied by spatially lateral inhomogeneous BHs and potential fluctuations at the interface.

4. Conclusion

The *I–V* characteristics of the Au/n-GaAs Schottky diodes quite well obey the TE current model introducing a Richardson constant value of 8.92 A cm^{-2} K^{-2}in the temperature range of 80–200 K which is in very close agreement with the known value of 8.16 A cm^{-2} K^{-2} for n-type GaAs. The decrease in the BH with a decrease in the temperature below 200 K has been attributed to the inhomogeneity of the contact. The barrier inhomogeneity assumption is also confirmed by the linear relationship between the barrier height and the ideality factor. Furthermore, it has been seen that the decrease in the experimental BH value obeys to GD model of BH based on the standard TE current theory according to Tung's Model in the temperature range of 80–200 K. It has been found that the value of σ_T=7.41 × 10^{-5} $cm^{2/3}$ $V^{1/3}$is in close agreement with σ_T=7.95 × 10^{-5} $cm^{2/3}$ $V^{1/3}$ value from the Φ_{eff} versus $(2kT)^{-1}$ curve in the range of 80–200 K. The modified Richardson plot according to Tung's model has given a Richardson constant value of 8.47 A cm^{-2} $K^{-2}$by considering effective area of the patches in temperature range of 80–200 K. Thus, we have concluded that the involved effective area of the patches in the current transport at low temperatures should be considered in calculation of the Schottky barrier diode parameters. Thereby, it has been concluded that Tung's lateral inhomogeneity model in the MS Schottky contacts is a convenient model when Schottky barrier inhomogeneity is responsible mechanisms for the abnormal behaviors in SBH, ideality factor and Richardson plots with a decrease in the temperature.

Acknowledgements

This work was supported by the Turkish Scientific and Technological Research Council of Turkey (TUBITAK). The authors also thanks to TUBİTAK and Hakkari University.

References

[1] E.H. Rhoderick, R.H. Williams, Metal–Semiconductor Contacts, 2nd ed., Clarendon, Oxford, 1988.
[2] S.M. Sze, Physics of Semiconductor Devices, 2nd ed., Willey, New York, 1981.
[3] S. Karatas, F. Yakuphanoglu, F.M. Amanullah, J. Phys, Chem. Solid 73 (2012) 46.
[4] B. Keskin, C. Denktas, A. Altındal, U. Avcıata, A. Gul, Polyhedron 38 (2012) 121.
[5] S. Tongay, T. Schumann, A.F. Hebard, Appl. Phys. Lett. 95 (2009) 22103.
[6] O.S. Anilturk, R. Turan, Solid-State Electron. 44 (2000) 41.
[7] C. Kenney, K.C. Saraswat, B. Taylor, P. Majhi, IEEE Trans. Electron Devices 58 (8) (2011) 2423.
[8] B.K. Sehgal, V.R. Balakrishnan, R. Gulati, S.P. Tewari, J. Semicond. Technol.. Sci. 3 (2003) 1.
[9] Y.P. Song, R.L. VanMeirhaeghe, W.H. Lafl ére, F. Cardon, Solid-State Electron. 29 (1986) 633.
[10] J.H. Werner, H.H. Guttler., J. Appl. Phys. 69 (3) (1991) 1522.
[11] J.P. Sullivan, R.T. Tung, M.R. Pinto, W.R. Graham, J. Appl. Phys. 70 (12) (1991) 7403.
[12] R.T. Tung, Phys. Rev. B: Condens. Matter 45 (1992) 13509.
[13] S. Chand, J. Kumar, J. Appl. Phys. 80 (1) (1996) 288.
[14] F. Iucolano, F. Roccaforte, F. Giannazzo, V. Raineri, J. Appl. Phys. 102 (2007) 113701.
[15] F. Roccaforte, F. La Via, V. Raineri, R. Pierobon, E. Zanoni, J. Appl. Phys. 93 (11) (2003) 9137.
[16] M. Kumar, B. Roul, T.N. Bhat, M.K. Rajpalke, A.T. Kalghatgi, S.B. Krupanidhi, J. Nanomater. 2011 (2011) 189731.
[17] M. Gulnahar, H. Efeoglu, J. Alloys Compd. 509 (2011) 7317.
[18] M. Soylu, F. Yakuphanoglu, J. Alloys Compd. 506 (2010) 418.
[19] A.A. Talin, R.S. Williams, B.A. Morgan, K.M. Ring, K.L. Kavanagh, Phys. Rev. B: Condens. Matter 49 (23) (1994) 16474.
[20] T. Tunc, S. Altindal, I. Uslu, I. Dokme, H. Uslu, Mater. Sci. Semicond. Process 13 (2010) 339.
[21] A.S. Kavasoğlu, O. Birgi, N. Kavasoğlu, G. Oylumluoğlu, A.O. Kodolbaş, R. Kangi, O. Yılmaz, J. Alloys Compd. 509 (2011) 9394.
[22] E. Dobrocka, J. Osvald, Appl. Phys. Lett. 65 (1994) 575.
[23] Zs.J. Horvath, Solid State Elecron. 39 (1) (1996) 176.
[24] J. Osvald, Zs.J. Horvath, Appl. Surf. Sci. 234 (1–4) (2004) 349.
[25] M. Yeganeh, Sh. Rahmatallahpur, R.K. Mamedov, Mater. Sci. Semicond. Process 14 (2011) 266.
[26] B. Gunduz, I.S. Yahia, F. Yakuphanoglu, Microelectron. Eng. 98 (2012) 41.
[27] Ş. Karataş, Ş. Altındal, Mater. Sci. Eng. B 122 (2) (2005) 133.
[28] I. Ay, H. Tolunay, Solid State Electron. 51 (2007) 381.
[29] L. Shen, H.W. Du, H. Ding, J. Tang, Z.Q. Ma, Mater. Sci. Semicond. Process. 14 (2011) 139.
[30] H. Norde, J. Appl. Phys. 50 (1979) 5052.
[31] S.K. Cheung, N.W. Cheung, Appl. Phys. Lett. 49 (1986) 85.
[32] N. Kwietniewski, M. Sochacki, J. Szmidt, M. Guziewicz, E. Kaminska, A. Piotrowska, Appl. Surf.Sci. 254 (2008) 8106.
[33] A. Turut, Turk. J. Phys. 36 (2012) 235.
[34] M. Missous, E.H. Rhoderick, D.A. Woolf, S.P. Wilkes, Semicond. Sci. Technol. 7 (1992) 218.
[35] R. Passler, Phys. Rev. B: Condens. Matter 66 (2002) 085201.
[36] C.D. Thurmond, J. Electrochem. Soc. 122 (1975) 1133.
[37] P. Lautenschlager, M. Garriga, S. Logothetidis, M. Cardona, Phys. Rev. B: Condens. Matter 35 (1987) 9174.
[38] S.Y. Zhu, C. Detavernier, R.L. Van Meirhaeghe, F. Cardon, G-P. Ru, X-P. Qu, B-Z. Li, SolidState Electron. 44 (2000) 1807.
[39] R.F. Schmitsdorf, T.U. Kampen, W. Mönch, J. Vac. Sci. Technol. B15 (1997) 1221.
[40] K. Akkılıç, M.E. Aydın, A. Turut, Phys . Scr.. 70 (2004) 364.
[41] W.P. Leroy, K. Opsomer, S. Forment, R.L. Van Meirhaeghe, SolidState Electron. 49 (2005) 878.